Pure appl. geophys. 162 (2005) 2095–2110
0033–4553/05/112095–15
DOI 10.1007/s00024-005-2706-7

© Birkhäuser Verlag, Basel, 2005

Pure and Applied Geophysics

Subsidence and Stress Change in the Cerro Prieto Geothermal Field, B. C., Mexico

E. Glowacka[1], O. Sarychikhina[1], and F. A. Nava[1]

Abstract—Previous works have shown that ground deformation and seismicity in the Cerro Prieto geothermal field (CPGF) are due to both tectonics and field exploitation. Here, we use information about current tectonics and data from precision leveling surveys, to model tectonic and anthropogenic subsidence. Our results show that tectonic subsidence constitutes only ~4% of the measured subsidence. Anthropogenic subsidence was evaluated using a model of rectangular tensional cracks, based on the hydrological model of the field, together with the Coulomb 2.0 program. From the resulting values of the fissure parameters and from extraction and injection data, we calculate that the volume changes caused by closure of the geothermal and cold water reservoirs account for only ~3% and ~7%, respectively, of the volume change which should occur due to extraction. Since 18% of the extracted fluids are reinjected, external recharge must compensate for about 72% of the expected volume reduction. An analysis of the changes in Coulomb stress caused by exploitation of the geothermal field suggest that even though the anthropogenic stresses account for only a fraction of tectonic stresses, they are large enough to trigger seismicity.

Key words: Cerro Prieto geothermal field, subsidence modeling, tectonic subsidence, anthropogenic subsidence, Coulomb stress changes.

Introduction

It is widely known that geothermal field exploitation can be accompanied by ground deformation (e.g., Wairakei, New Zealand (Allis *et al*, 1998); Geysers, U.S.A. (Mossop and Segall, 1997)). Since the energy per unit mass of geothermal water is relatively small compared with that from oil or coal, geothermal energy production involves extraction of large volumes of water. A drastic reduction of underground water is partially compensated by a reduction of the volume of the

[1] CICESE. International address: PO Box 434843, San Diego, CA, 92143-4843, U.S.A. National address: km 107 Carretera Tijuana-Ensenada, Apdo. Postal 2732, Ensenada, B.C., Mexico.
E-mail: glowacka@cicese.mx, osarytch@cicese.mx, fnava@cicese.mx

reservoir. Also, fluid extraction cools the reservoir, causing further volume reduction and deformation. There is ample evidence that the effects of reservoir deformation propagate to the ground surface, causing both vertical and horizontal ground displacement. Additionally, the strains caused by the volume decrease of the reservoir may cause slip along faults, leading to activation of seismicity (NARASIMHAN and GOYAL, 1984). Seismicity induced by geothermal fluid extraction has been reported for Geysers, U.S.A. (EBERHART-PHILLIPS and OPPENHEIMER, 1984) and Coso, U.S.A. (FIALKO and SIMONS, 2000).

The Cerro Prieto geothermal field (CPGF) is located in northern Baja California, Mexico, to the south of Mexicali, in the southern portion of the Salton basin which is considered to be one of the geological provinces with the largest geothermal resources in the world (Fig. 1). The field is operated by the Mexican Federal Electricity Commission (Comisión Federal de Electricidad, CFE). Cerro Prieto is a high-temperature, fluid-dominated, geothermal field, contained in sedimentary rocks. The geothermal fluid, with a temperature of 250°–350°C, is extracted from gray shales, isolated from the unconsolidated rock by a layer of mudstone and brown

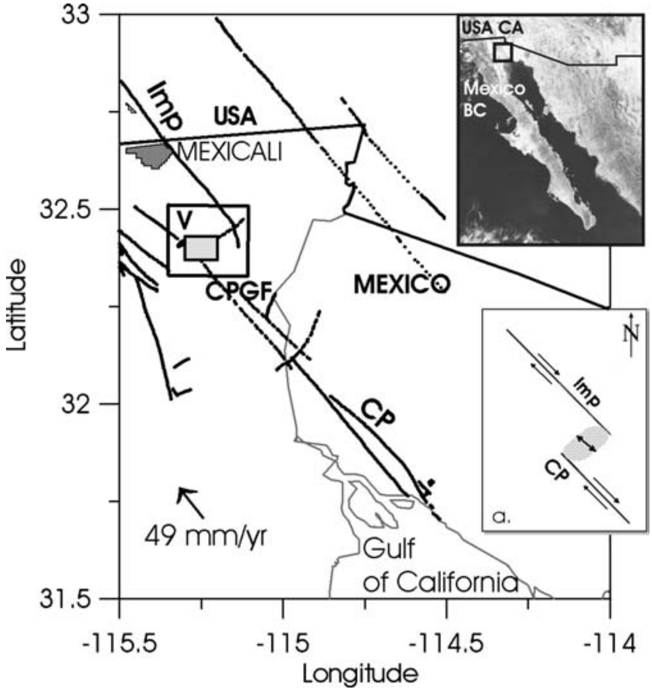

Figure 1
Location map. CPGF — Cerro Prieto Geothermal Field (small, grey rectangle), Large rectangle — study area, Imp — Imperial fault, CP — Cerro Prieto fault, V — Cerro Prieto volcano, (a) Schematic presentation of the pull-apart basin.

shales which constitutes the cap-rock. A geologic cross section of the vicinity of the CPGF (CFE, 1995) shows a thick sedimentary filled basin, with unconsolidated sediments occupying more than 2 km, and sedimentary layers of mudstone and shales lying below. Sedimentary rocks are disturbed and displaced by normal faults, and tilted as an effect of local tectonics. The CPGF reservoir is characterized by having "leaky" boundaries where the hot geothermal fluids exist in dynamic equilibrium with much cooler waters (TRUESDELL and LIPPMANN, 1990). It is generally accepted that the field is recharged from the east by hot water, and from east, west and south as well as from above (TRUESDELL *et al.*, 1998) by colder water from shallow aquifers of the alluvial basin of the Colorado River. Figure 1 presents the geographical and tectonic state of the discussed area.

Fluid extraction for electricity production began in 1973 at 1500–3000 m depths. Currently, the CPGF is the world's second largest geothermal field with a 720 MW capacity. Reinjection of residual water began in 1989, and currently about 20% of the extracted fluid is being reinjected at 500–2600 m depth.

The CPGF is located within an extremely active tectonic region, in the boundary between the Pacific and North American plates, consisting of a wide zone of transform faults from the San Andreas system with relative interplate motion of 4.9 cm/y (BENNETT *et al.*, 1996). The CPGF lies in a pull-apart basin, created between the Imperial and Cerro Prieto faults, both with NW-SE strike and right-lateral motion, and is characterized by a high level of seismicity and tectonic deformation. The CPGF area, located near the northern end of the Cerro Prieto fault and the area near the southern end of the Imperial fault, is dominated by seismic swarms, while strong main shocks ($M \geq 6$) occur along the traces of these faults (FREZ and GONZÁLEZ, 1991). The possibility that fluid extraction and injection in the Cerro Prieto Geothermal Field (CPGF) is stimulating seismicity in the Mexicali Valley has been mentioned before (MAJER and MCEVILLY, 1982; GLOWACKA and NAVA, 1996; FABRIOL and MUNGUÍA, 1997).

Subsidence at the CPGF is related not only to its particular tectonic setting, since there is evidence that part of its observed subsidence is induced by fluid extraction. During 1977–1997 the subsidence rate at the center of the field increased after each large production increase (GLOWACKA, *et al.*, 1999). The area of maximum subsidence (12 cm/yr) coincides with that of the extraction wells, and this subsidence rate is too high to be caused by tectonic activity alone. These facts suggest that subsidence in the CPGF is caused mainly by fluid extraction. Subsidence at CPGF was also measured by SAR (Synthetic Aperture Radar) interferometry by CARNEC and FABRIOL (1999) and HANSSEN (2001) and was interpreted as being produced by geothermal fluid extraction.

The present works aim to model both the tectonic and the anthropogenic parts of the observed subsidence, and to evaluate the stress changes caused by the anthropogenic component and compare them to the seismotectonic stresses in the study area.

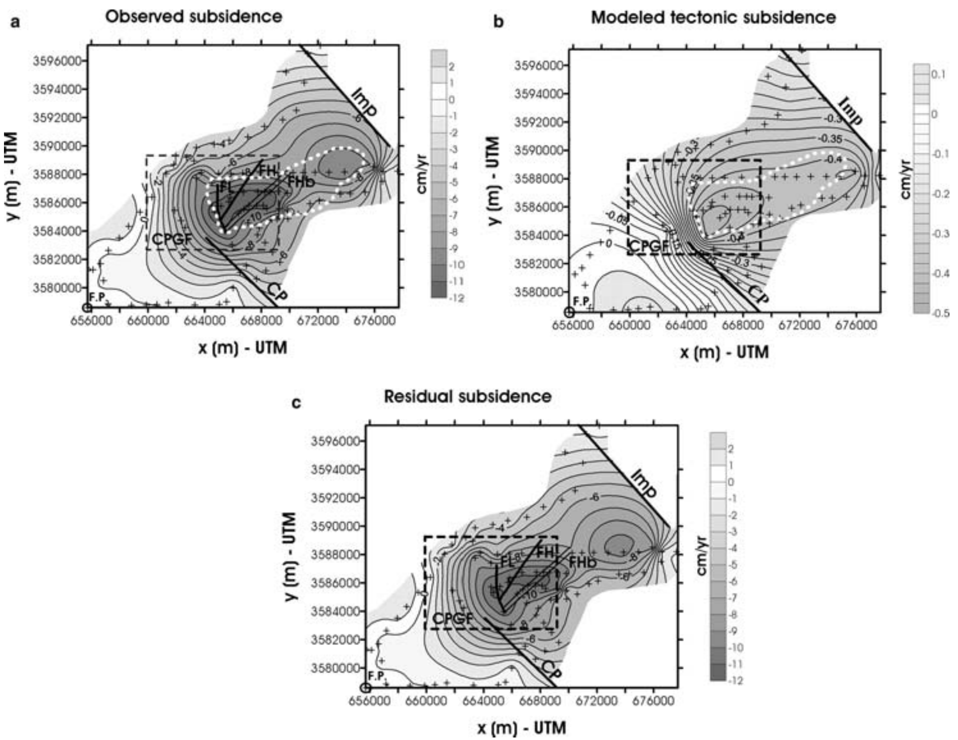

Figure 2

(a) Observed subsidence rate (1994–1997) in cm/yr. Rectangle — CPGF. Dotted line — T ≥ 300° isotherm. Crosses — leveling points. F. P. — fixed point. FH — surface projection of H fault. FHb — intersection of H fault with the ceiling of the β reservoir, FL — L fault. (b) Modeled tectonic subsidence in cm/yr; rate relative to the fixed point. (c). Difference between observed and tectonic subsidence.

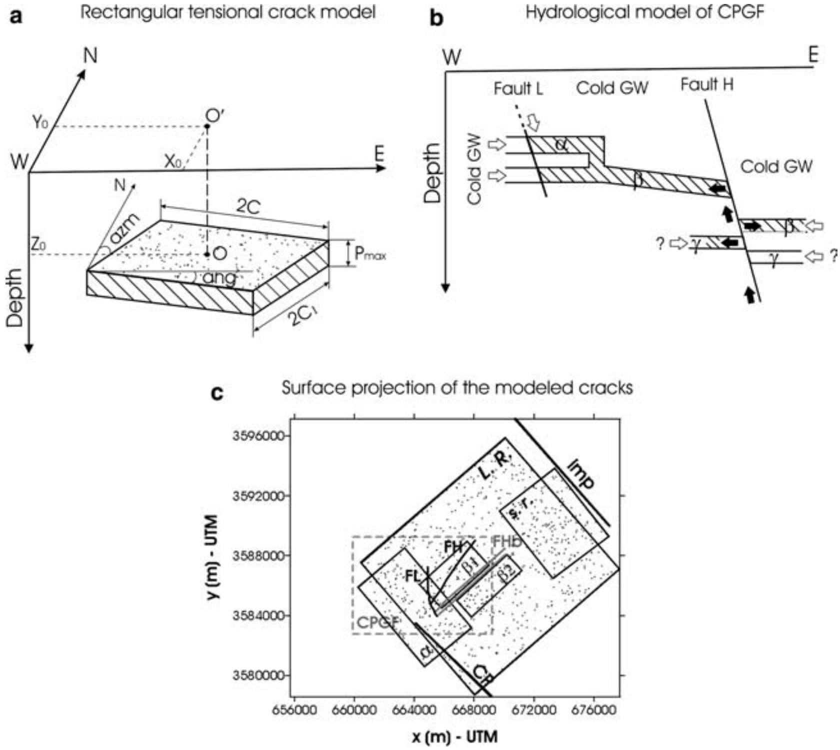

Figure 3

Modeling of anthropogenic subsidence. (a) Rectangular tensional crack (modified from YANG and DAVIS, 1986). (b) Hydrological model, modified from LIPPMANN *et al.*, (1991). Black and white arrows indicate hot and cold water flow, respectively. (c) Surface projection of modeled cracks.

Data

We use the leveling data published in GLOWACKA *et al.* (1999). The data were recorded during the 1994–1997 period by CFE (LIRA and ARELLANO, 1997) and CICESE (GLOWACKA *et al.*, 1999). The leveling reference point is located in the SE part of the area, in the Cucapah Mountains, and is assumed to be stable. The subsidence rate is shown in Figure 2 (a). The dominant feature is the elliptical area with the highest subsidence rate, oriented NE-SW. This area agrees with the boundary of the geothermal anomaly. The maximum subsidence rate of ~12 cm/yr is located at the center of the extraction zone; while another, local, maximum with a subsidence rate ~9 cm/yr is located to the NE of the field. The second maximum was interpreted as a fluid recharging area of the geothermal field (GLOWACKA *et al.*, 1999).

Using the approach published in DZURISIN *et al.* (2002), SARYCHIKHINA (2003) estimated a subsidence rate uncertainty of 0.34 cm/yr. This estimation includes two components: the leveling error, which depends on the distance between stations, and the error due to benchmark instability.

The role of faults located in the extraction zone was analyzed by LIPPMANN *et al.* (1991). According to these authors, faults H and L (Fig. 2a) are used as a conduct for hot and cold water recharging and as boundaries between reservoirs α, β and γ (Fig. 3b).

The Cerro Prieto fault, which crosses the CPGF area in a series of small scarps and cracks, was surveyed by CFE between 1995 and 1998, and 4 cm/year east side down displacement was observed for this period (LIRA, 1999). Since 1996, an extensometer installed in the southernmost part of Imperial fault has recorded an average 6 cm/year vertical displacement across the fault (along the 3 m span of extensometer). Analyzing extension, amplitude, and time behavior of the slip on the Imperial and Cerro Prieto faults which bound the Cerro Prieto pull-apart basin from the NE and SW, GLOWACKA *et al.* (1999, 2005) suggest that these faults constitute a boundary of the subsided area, and probably are the groundwater barrier.

Tectonic Subsidence Modeling

The CPGF is located between the Imperial and Cerro Prieto faults, two major strike-slip, right-lateral, step-over to the right faults; faults responsible for the natural subsidence in the studied area because they create a pull-apart zone (Fig. 1a). Since there were no subsidence measurements before extraction began, the only way to estimate the tectonic subsidence is by modeling. We evaluate the vertical deformation caused by the right-lateral motion between the North American and Pacific plates. We consider horizontal displacement rates of 3.5 cm/yr for the Imperial fault and 4.2 cm/yr for the Cerro Prieto fault (BENNETT *et al.*, 1996). We used these displacement rates as an approximation of the long-term effect of shearing and pulling in the pull-apart center because they are larger than the displacement estimated from seismic moments over the time of this study (SARYCHIKHINA, 2003).

Since earthquakes in the study area occur within the top 15 km (GLOWACKA *et al.*, 1999; REBOLLAR *et al.*, 2003), we assumed that the Imperial and Cerro Prieto faults extend from the surface to this depth, and that the upper crust is elastic. The focal mechanisms of earthquakes with magnitude $M > 5$ show that these faults are vertical with right-lateral motion (FREZ and GONZÁLEZ, 1991). In order to locate the northern tip of the Cerro Prieto fault, and the southern tip of the Imperial fault, we used the data from GONZÁLEZ *et al.* (1998) and GPS field measurements. To calculate the subsidence we used the Coulomb 2.0 program (KING *et al.*, 1994; TODA *et al.*, 1998). The program implements the elastic dislocation formulae of OKADA (1992) and the boundary element formulae of CROUCH and STARFIELD (1983).

The tectonic subsidence rate relative to the reference point is shown in Figure 2b. The maximum subsidence rate (0.45 cm/yr) coincides with the CPGF area, while the northeastern anomaly coincides with the previously defined recharging area. According to our results, tectonic subsidence accounts for only ~4% of the total observed subsidence.

It should be mentioned that, since the value of Poisson's coefficient is not precisely known for the study region, tectonic subsidence was calculated using a constant 0.25 value. GUPTA *et al.* (1982) showed that, within the Geysers geothermal field, Poisson's coefficient can vary by about 0.05. Such a variation, if applied to CPGF, changes our calculated subsidence rate by ~0.05 cm/yr, which does not effect our conclusions.

We did not take into account the compaction and isostasy effects that can influence the modeled subsidence rate. We estimate, from published works on compaction (CARILLO, 2003) and isostasy (CONTRERAS *et al.*, 1997; GARCÍA ABDESLEM, 2003) that these processes together can increase the tectonic subsidence rate by at most 40% of the estimated rate. Even if this additional rate is taken into account, the tectonic subsidence rate in CPCF is still of the order of millimeters per year.

The estimated tectonic subsidence is of the order of those calculated for nearby areas using other methods: 0.16 cm/yr for Laguna Salada, 20 km west of Mexicali (CONTRERAS *et al.*, 2002) and 0.55 cm/yr for the Vallecito-Fish Creek basin 50 km north of Mexicali (JOHNSON *et al.*, 1983).

The geometry of the tectonic subsidence could probably explain the location of the geothermal field, because in the zones of maximum subsidence an increment in heat flow can be expected, due to the thinning of the crust caused by the vertical deformation. Also, since the zone of maximum subsidence has the thickest sediment accumulation, it will have the largest anthropogenic subsidence when extraction takes place. Therefore, as has been concluded in GLOWACKA *et al.* (2003), the similarity between Figures 2a and 2b can be explained by a dominant tectonic control on the origin of geothermal field and sedimentation process. A similar situation was described for the San Joaquin valley in California (BULL, 1998), where the extent and magnitude of land subsidence caused by water extraction reflects pervasive tectonic control on depositional processes along the Pacific-North American plate boundary.

Anthropogenic Subsidence Modeling

Mathematical models used for vulcanology and hydrofracturing can be applied to evaluating the elastic deformation caused by volume extraction. The one most commonly used is the MOGI (1958) model of a spherical source with hydrostatic pressure, embedded in an elastic half-space. This model was used by MOSSOP and SEGALL (1997) to model subsidence in the Geysers geothermal field, and by CARNEC and FABRIOL (1999) and HANSEN (2001) to model subsidence in the CPGF. The model of deflation of a triaxial ellipsoidal cavity in an elastic half-space (DAVIS, 1986) was used for subsidence modeling in the Coso geothermal

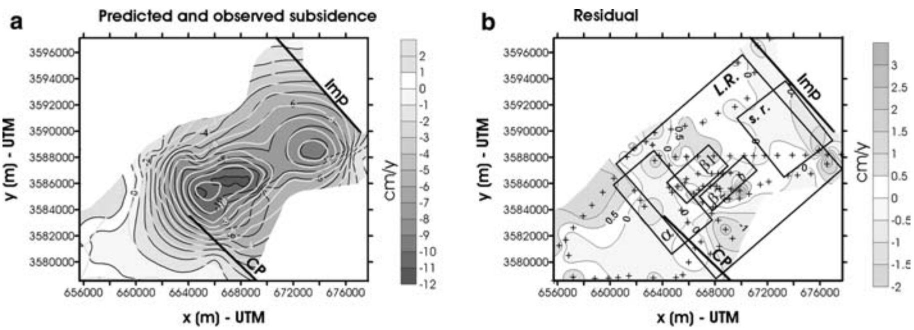

Figure 4
Results of modeling. (a) Black isolines are observed subsidence rate (minus tectonic component), white isolines are modeled. (b) Residuals (cm/yr).

Table 1

Model fracture parameters

Fracture	Parameters							
	Center (m)			(m)			(°)	
	x	y	z	p	c1	c	azm.	ang.
α	664032	3584530	1100	−0.05	3471.5	2019	140	1
β_1	666667	3586700	2100	−0.1	1099	2144	138	4
β_2	669000	3586000	2250	−0.12	737.5	2293	138	4
s.r.	673352	3590150	1500	−0.079	2907	2333.5	142	7
L. R.	669057	3587291	996	−0.04	5806	6347.5	139	1

field (FIALKO and SIMONS, 2000). The subsidence induced by fluid extraction was evaluated by SEGALL (1989) and WALSH (2002) using a poroelastic model of an axisimmetric reservoir. All these models have some kind of symmetry, two- or three-dimensional, and no tilt dependence. Because the CPGF reservoirs are located in tilted sedimentary layers and bounded by faults, we decided to use the mathematical model of a rectangular tension crack (YANG and DAVIS, 1986) as the one which better represents the geometry of reservoirs. Each crack is characterized by the parameters: x, y, z (center of crack), p (crack closure), c and $c1$ (half-crack length and width dimensions), and azimuth and dip (crack orientation) (Fig. 3a).

We proceeded to model the anthropogenic component of subsidence, subtracting the calculated tectonic component from the observed subsidence (Fig. 2c); although SARYCHIKHINA (2003) showed that inclusion of tectonic subsidence does not significantly change the modeling results.

Table 2

Volume change cause by crack closure

Fracture	Volume change (m^3/yr)	
α	1.4×10^6	3.2×10^6
β_1	1×10^6	
β_2	0.8×10^6	
s.r.	2.1×10^6	8.1×10^6
L.R.	6×10^6	
Total	1.1×10^7	

Modeling was done using the Coulomb 2.0 program. Three closing cracks were positioned according to a hydrologic model of the field which consists of two heavily exploited reservoirs: α and β (HALFMAN *et al.*, 1984; LIPPMANN *et al.*, 1991). β reservoir is divided by the normal SE dipping fault *H* (Figs. 2a and 3b,c) into two blocks: upper (β_1) and lower (β_2). One small crack was placed under the center of the secondary subsidence center (s. r. — small recharge), and a large one (L. R. — large recharge) was placed above the reservoirs that extend under a large part of the study area, in order to produce the observed subsidence outside the CPGF (Fig. 3c). Modeling was done by trial and error, and the resulting crack parameters are shown in Table 1.

A comparison of anthropogenic observed versus modeled subsidence rates is shown in Figure 4a, and the residual is shown in Figure 4b. Both shape and magnitude of the modeled subsidence rate are quite similar to the observed ones; the absolute value of the residual at most observation points is about 0.0 to 0.5 cm/yr, although local discrepancies show as much as 2.5 cm/yr (Fig. 4b).

The root-mean-square error per observation point (RMS) of this model is 0.79 cm/yr. It is possible to reduce the RMS using very small cracks to eliminate the local anomalies, but in most cases these anomalies are due to a single point and may represent measurement errors. After parameter adjustment to fit the observed subsidence rate, the model is in good agreement with the hydrological model on which it was based.

Recharged Volume

In the following calculations we assumed that the change in volume of every particular crack is equivalent to the volume removed from (or added to) the crack. We do not take into account cooling, and do not delve into the physics of the compaction processes which take place in the reservoir. With this assumption, using the estimated values of the crack dimensions and their closures, we evaluate the volume change in the reservoirs, shown in Table 2. If we compare this change with the rate of net extraction (extraction minus injection), we can estimate the volume of external recharge. For 1994–1997, the average extraction rate is 1.05×10^8 ton/yr, (or 1.05×10^8 m^3/yr, assuming that 1 ton is roughly equivalent to 1 m^3 of geothermal fluid), 18% of which (1.88×10^7 ton/yr) has been reinjected. Thus, the crack-induced change of volume corresponds to only ~10% of the volume decrease expected from

Table 3

Regional stresses

Principal stresses	Orientation	Magnitude (bar)	Reference
σ_1	N5° E	100	1. STEIN *et al.*, 1992
σ_2	Vertical	50	2. FUIS *et al.*, 1982
σ_3	N85° W	0	

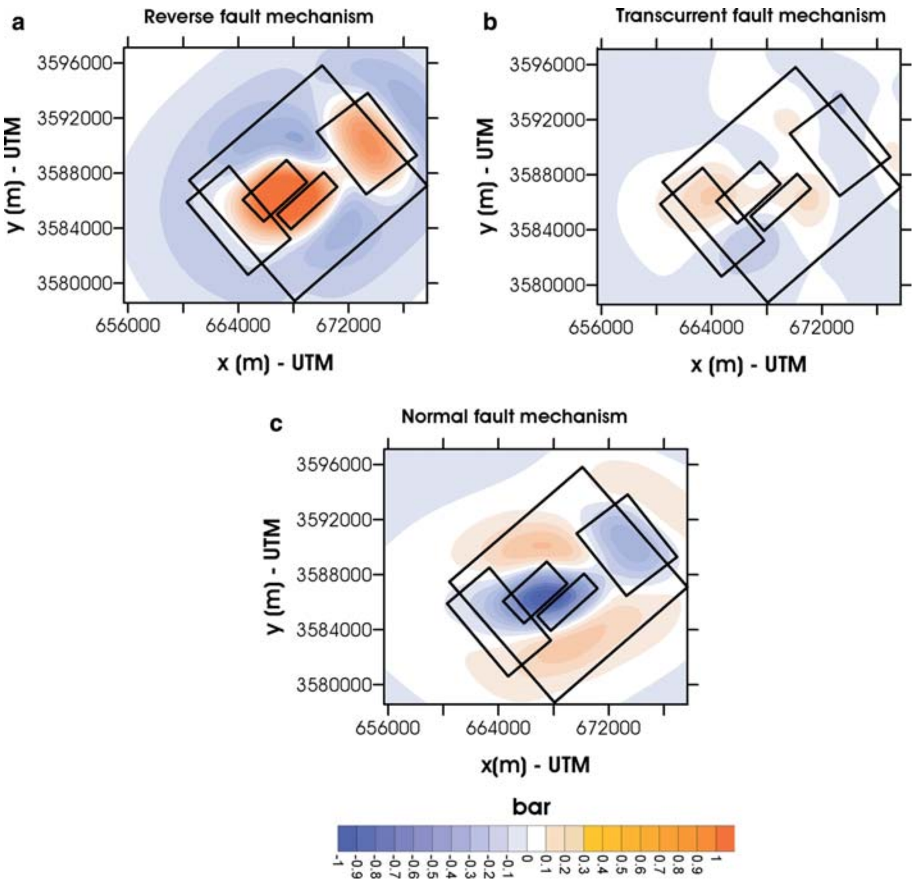

Figure 5

Coulomb stress change at 6 km depth caused by the modeled crack closure for various optimally oriented faults: (a) — Reverse, (b) — Transcurrent, (c) — Normal fault mechanism.

the extraction figures. Of this 10%, only 3% is caused by volume decrease in the hot water reservoirs, while 7% is due to volume decrease in the cold water reservoirs.

Since reservoir volume decrease accounts for only 10% of the extracted volume, and injection volume accounts for 18%, it follows that 72% of this volume is compensated by recharge from the deep, regional aquifer proposed in PELAYO *et al.* (1991) and GLOWACKA and NAVA (1996). Unfortunately, this recharge zone cannot be modeled using our data set because it is considerably larger than the leveling network. The recharge volume of the present work is comparable to those from recharge evaluation using a poro-elastic model (GLOWACKA and NAVA, 1996), but contradict the assumption that all extraction volume is recharged (PELAYO *et al.*, 1991).

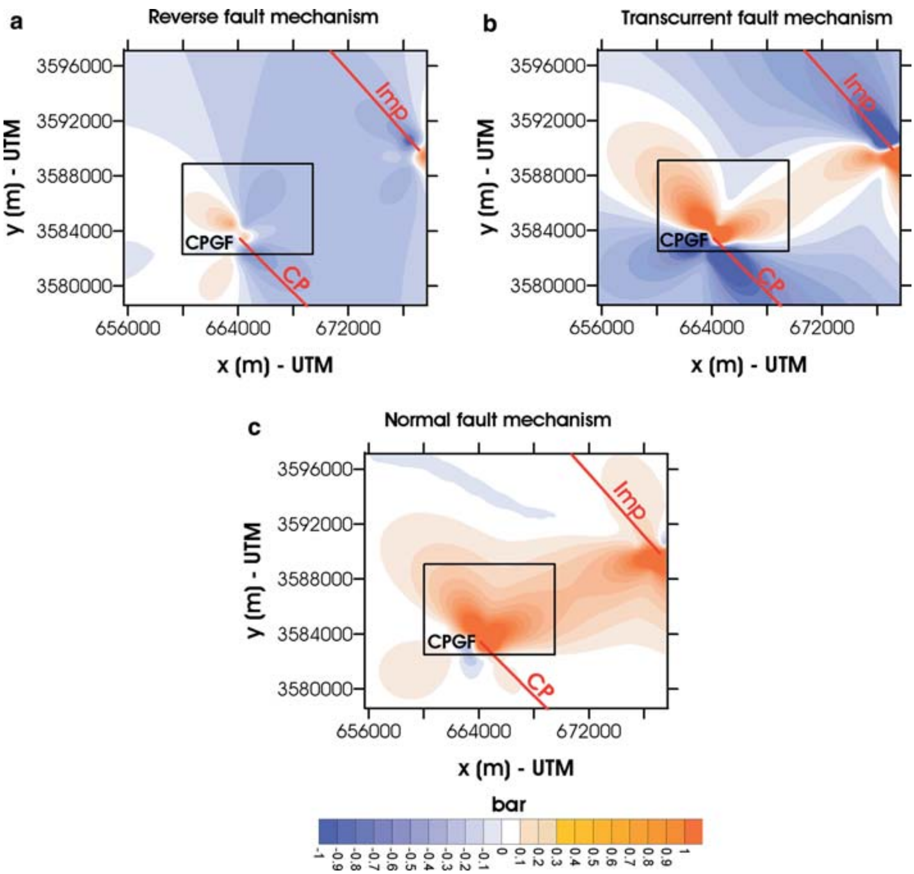

Figure 6

Coulomb stress change caused by slip along the Imperial and Cerro Prieto faults for (a) — Reverse, (b) — Transcurrent, (c) — Normal fault mechanism.

Table 4

Change in Coulomb stress (bar/yr)

Fault mechanism	Tectonic faults		Model cracks	
	minimum	maximum	minimum	maximum
Strike-slip	−3.2	3.6	−0.2	0.3
Normal	−0.3	4.0	−1.0	0.4
Reverse	−1.1	1.1	−0.4	1.7

Stress Changes and Seismicity

Deformation caused by fluid extraction in geothermal reservoirs produces stress changes that may be capable of triggering earthquakes (Segall *et al.*, 1994). As determined above, 96% of the observed subsidence at the CPGF is due to reservoir fluid extraction, and it is important to assess how much this anthropogenic activity changes the stress field and influences seismicity in the area, as compared with the stress change caused by tectonic motion.

The most commonly-used stress formulation is the static Coulomb failure stress (Stein *et al.*, 1992). All Coulomb stresses were calculated using the Coulomb 2.0 program and a friction coefficient $\mu' = 0.4$ (Stein *et al.*, 1992). The applied regional stress magnitude and orientation found for Southern California by Fuis *et al.* (1982) and Stein *et al.* (1992), are shown in Table 3. To calculate the changes in Coulomb stress caused by interplate motion, we used the same assumptions as for calculating tectonic subsidence. We will denote as *CSCA* and *CSCT* the Coulomb stress change caused by anthropogenic activity and by tectonics, respectively.

Seismicity in the CPGF area is reported to occur in the 1–15 km depth range, and the maximum number of earthquakes occurs in the 4–6 km depth range (Glowacka *et al.*, 1999). We calculated the *CSCA* for the 1–8 km depth range. The *CSCA* caused by closure of model cracks for different fault types at 6 km is shown in Figure 5. We obtained the increase in stress for reverse faulting both above and below the reservoir, and for normal and transcurrent faulting at the margins of the studied area. These results are similar to those obtained by Segall (1989) for oil and gas fields, where he modeled ground deformation caused by extraction using a poro-elastic model.

Since we have assumed uniform slip across the fault width, from the surface to 15 km depth, the change in Coulomb stress caused by motion along the tectonic faults is the same over this depth range. Figure 6 shows the CSCT for different faulting mechanisms. The maximum CSCT occurs for normal faulting (Fig. 6c) in the area between the faults. In this area, stresses are relaxed for reverse faulting (Fig. 6a) and increased for strike-slip faulting (Fig. 6b). The CSCT and CSCA maximum and minimum values for 6 km depth are listed in Table 4. The maximum values of CSCA are at least 0.1 bar/year, for all faulting types, and represent 10%–17% of the maximum tectonic stress changes.

According to our results, thanks to recharge and injection, only 10% of extracted volume is responsible for the observed subsidence, and creates anthropogenic CSCA of the order of 10% of tectonic CSCT. Thus the process of recharge not only guarantees longevity to the CPGF, but also diminishes the potential for subsidence as well as the effects of deformation on the stress field. However, the same process causes subsidence to effect an area which is considerably larger than that analyzed in this work (but which we cannot quantify because of the lack of leveling data) so that, as proposed in GLOWACKA and NAVA (1996), it may influence seismicity at distances substantially larger than those considered.

If the assumption that the volume change is produced by extraction only, and not by thermal contraction, is not true, then the estimated volume extracted from the CPGF area is actually an upper bound. This does not change our results about *CSCA*, however the area which can be effected by subsidence and seismicity is larger.

Conclusions

During 1994–1997, tectonic induced subsidence with a maximum value of 0.45 cm/yr accounts for only 4% of the observed subsidence at the CPGF and surrounding area. We modeled the anthropogenic subsidence using tensional rectangular cracks: Two corresponding to cold aquifers and three corresponding to geothermal reservoirs. The crack positions agree with the hydrological model of the field. Under the assumption presented in this work, the volume change produced by the closure of the reservoir cracks accounts for only ~3% of the extracted volume, while 7% of this volume is due to volume decrease in the cold water reservoirs. Considering that injection is about 18% of extraction, it evenuates that about 72% of the extracted volume must be compensated by water from an external aquifer larger than the study area.

An analysis of the Coulomb stress changes indicates that, in the natural state, seismicity in the area is dominated by normal and transcurrent earthquakes; a well-known behavior of pull-apart basins. Under fluid extraction conditions, Coulomb stress increases by more than 0.1 bar/yr, for all faulting types. According to HARRIS (1998), a Coulomb stress change as low as 0.1 bar can trigger an earthquake. Hence, the stress change caused by extraction could trigger earthquakes of all types; this supports the possibility that some seismicity at the CPGF might be triggered by fluid extraction, as proposed by MAJER and MCEVILLY (1982) and GLOWACKA and NAVA (1996).

Acknowledgements

The results and conclusions presented in this work are solely the authors and do not necessarily express the points of view of CFE. The authors are grateful to Jose

Romo, Juan Contreras and Modesto Ortiz Figueroa for criticism and discussion during the work on this project. This work greatly benefited from the comments offered by two anonymous reviewers.

This research was sponsored in part by CONACYT, project number 35183-T and CICESE internal funds.

References

Allis, R.G., Zhan, X., and Clotworthy, A. (1998), *Predicting Future Subsidence at Wairakei Field, New Zealand*, Geothermal Resources Council Trans. *22*, 43–47.

Bennett, R.A., Rodi, W., and Reilinger, R.E. (1996), *Global Positioning System Constrains on Fault Slip Rates in Southern California and Northern Baja, Mexico*, J. Geophys. Res. *101* (B10), 21,943–21,960.

Bull, W.B., *Tectonic controls of geomorphic processes in land subsidence area*. In *Land Subsidence* (ed. J.W. Borchers) (Star Publishing Company 1998), pp. 29–37.

Carillo, R.M., *Palinoestratigrafia del neogeno en la cuenca Macuspana, Tabasco, México* (Tesis de Maestría, CICESE, México 2003).

Carnec, C. and Fabriol, H. (1999), *Monitoring and Modeling Land Subsidence at the Cerro Prieto Geothermal Field, Baja California, Mexico, Using SAR Interferometry*, Geophys. Res. Lett. *26*(9), 1211–1214.

CFE, *Cerro Prieto Geothermal Field* (CFE, Mexico 1995).

Contreras, J., Scholz, Ch.H., and King, G.C.P. (1997), *A model of Rift Basin Evolution Constrained by First-order Stratigraphic Observation*, J. Geophys. Res. *102*(B4), 7673–7690.

Contreras, J., Martin-Barajas, A., and Herguera, J.C. (2002), *Subsidence and Extensión Rates of Laguna Salada Basin, Northeastern Baja California, Mexico*, EOS Trans. AGU *83*(47), Fall. Meet. Supll., Abstract T52C – 1223, San Francisco.

Crouch, S.L. and Starfield A.M. *Boundary Element Method in Solid Mechanics* (Allen Unwin, London 1983) 322 pp.

Davis, P.M. (1986), *Surface Deformation due to Inflation of an Arbitrary Oriented Triaxial Ellipsoidal Cavity in an Elastic Half-space, with References to Kilauea Volcano, Hawaii*, J. Geophys. Res. *91*(B7), 7429–7438.

Dzurisin, D., Poland, M.P., and Burgmann, R. (2002), *Steady Subsidence of Medicine Lake Volcano, Northern California, Revealed by Repeated Leveling Surveys*, J. Geophys. Res. *107*(B12), 2372,8-1– 8–16.

Eberhart-Phillips, D. and Oppenheimer, D.H. (1984), *Induced Seismicity in The Geysers Geothermal Area, California*, J. Geophys. Res. *89*, 1191–1207.

Fabriol, H. and Munguía, L. (1997), *Seismic Activity at the Cerro Prieto Geothermal Area (Mexico) from August 1994 to December 1995, and Relationship with Tectonics and Fluid Exploitation*, Geophys. Res. Lett. *24*(14), 1807–1810.

Fialko, Y. and Simons, M. (2000), *Deformation and Seismicity in the Coso Geothermal Area, Inyo Country, California: Observation and Modeling Using Satellite Radar Interferometry*, J. Geophys. Res. *195*(B9), 21,781–21,793.

Frez, J. and González, J.J., *Crustal structure and seismotectonics of northern Baja California*. In *The Gulf and Peninsular Province of the Californias* (eds. Simoneit, B. and Dauphin, J.P.) (AAPG Memoir # 47, 1991), pp. 261–283.

Fuis, G.S., Mooney, W.D., Healey, J., McMechan, G.A., and Lutter, W.J., *Crustal structure of the Imperial Valley region*. In *The Imperial Valley. California Earthquake, October 15, 1979* (Geological Survey Professional Paper 1982), pp. 25–49.

Garcia Abdeslem, J. (2003), *3-D Numerical Model of the Flexural Isostatic Response to Extension Induced by Crustal Scale Listric Normal Faulting*, Geofísica Internacional *42*(1), 41–51.

Glowacka, E., Sarychikhina, O., and Nava, A. (2005), *A Genetic Algorithm in Subsidence Modeling in the Cerro Prieto Geothermal Field, Baja California, Mexico*. Proceedings, World Geothermal Congress 2005.

GLOWACKA, E., SARYCHIKHINA, O., and CONTRERAS, J. (2003), *Subsidence in the Cerro Prieto Field: Relation Between Tectonic and Anthropogenic Components*, Geothermal Resources Council Trans. *27*, 473–475.

GLOWACKA, E., GONZÁLEZ, J.J., and FABRIOL, H. (1999), *Recent Vertical Deformation in Mexicali Valley and its Relationship with Tectonics, Seismicity and Fluid Operation in the Cerro Prieto Geothermal Field*, Pure Appl. Geophy. *156*, 591–614.

GLOWACKA, E. and NAVA, F.A. (1996), *Major Earthquakes in Mexicali Valley, México, and Fluid Extraction at Cerro Prieto Geothermal Field*, Bull. Seismol. Soc. Am. *86*(1A), 93–105.

GONZÁLEZ, J.J., GLOWACKA, E., SUÁREZ, F., QUIÑÓNEZ, G., GUZMÁN, M., CASTRO, J.M., RIVIERA, F., and FELIX, M.G. (1998), *Movimiento reciente de la falla Imperial, Mexicali, B. C.*, Divulgare, Ciencia para todos, Mexicali, B. C. *6*(22), 4–15.

GUPTA, H.K., WARD, R.W., and TZEU-LIE, L. (1982), *Seismic Wave Velocity Investigation at the Geysers-Clear Lake Geothermal Field, California*, Geophysics *47*(5), 819–824.

HALFMAN, S.E., LIPPMANN, M.J., ZELWER, R., and HOWARD, J.H. (1984), *A Geologic Interpretation of the Geothermal Fluid Movement in Cerro Prieto Field, Baja California, Mexico*, Assoc. Pet. Geolog. Bull. *68*, 18–30.

HANSSEN, R.F., *Radar Interferometry* (Kluwer Academic Publisher, Netherlands 2001).

HARRIS, R.A. (1998), *Introduction to Special Section: Stress Triggers, Stress Shadows, and Implications for Seismic Hazard*, J. Geophys. Res. *103*(B10), 24,347–24,358.

JOHNSON, N.M., OFFICER, C.B., OPDYKE, N.D., WOODARD, G.D., ZEITLER, P.K., and LINDSAY, E.H. (1983), *Rates of late Cenozoic Tectonism in the Vallecito – Fish Creek Basin*, Geology *11*, 664–667.

KING, G.C.P., STEIN, R.S., and LIN, J. (1994), *Static Stress Changes and the Triggering of Earthquakes*, Bull. Seismolog. Soc. Am. *84*(3), 935–953.

LIPPMANN, M.J., TRUESDELL, A.H., MAÑÓN, A.M., and HALFMAN, S.E. (1991), *A Review of the Hydrogeologic-Geochemical Model for Cerro Prieto*, Geothermics *20*, 39–52.

LIRA, H., *Resultados del monitoreo de desplazamiento de la falla Cerro Prieto en 1998* (Informe Técnico RE05/99, CFE 1999).

LIRA, H. and ARELLANO, J.F., *Resultados de la nivelación de precisión realizada en 1997, en el campo geotérmico Cerro Prieto* (Informe técnico RE 07/97, CFE 1997).

MAJER, E.L. and MCEVILLY, T.V. (1982), *Seismological Studies at the Cerro Prieto Geothermal Field*, 1978–1982, Proc. Fourth Symp. on the Cerro Prieto Geothermal Field, Baja California, Mexico, Comisión Federal de Electricidad, 145–151.

MOGI, K. (1958), *Relations between the Eruptions of Various Volcanoes and the Deformation of the Ground Surface around them*, Bull. Earthq. Res. Inst. Univ. Tokyo *36*, 99–134.

MOSSOP, A.P. and SEGALL, P. (1997), *Subsidence at the Geysers Geothermal Field, N. California from a Comparison of GPS and Leveling Surveys*, Geophys. Res. Lett. *24*, 1839–1842.

NARASIMHAN, T.N. and GOYAL, K.P., *Subsidence due to geothermal fluid withdrawal, in Man – Induced land subsidence*. In *Rev. Engin. Geology 6* (ed. Holzer, T.L.) (Geol. Soc. Am., Boulder, Colorado 1984), pp. 35–66.

OKADA, Y. (1992), *Internal Deformation due to Shear and Tensil Faults in a Half-space*, Bull. Seismol. Soc. Am. *82*(2), 1018–1040.

PELAYO, A., RAZO, A., GUTIÉRREZ, L.C., ARELLANO, F., ESPINOZA, J.M., and QUIJANO, J.L., *Main geothermal field of Mexico; Cerro Prieto geothermal field, Baja California, The geology of North America*. In *Economic Geology, P-3* (ed. Salas G. P.) (Mexico, GSA 1991), pp. 23–57.

REBOLLAR, C.J., REYES, L.M., QUINTANAR, L., and ARELLANO, J.F. (2003), *Stress Heterogeneity in the Cerro Prieto Geothermal Field, Baja California, Mexico*, Bull. Seismol. Soc. Am. *93*(2), 1–12.

SARYCHIKHINA, O., *Modelación de subsidencia en el campo geotérmico Cerro Prieto* (Tesis de Maestría, CICESE, México 2003).

SEGALL, P. (1989), *Earthquakes Triggered by Fluid Extraction*, Geology *17*, 942–946.

SEGALL, P., GRASSO, J.-R., and MOSSOP, A. (1994), *Poroelastic Stressing and Induced Seismicity near the Lacq Gas Field, Southwestern France*, J. Geophys. Res. *99*(B8), 15,423–15,438

STEIN, R.S., KING, G.C.P., and LIN, J. (1992), *Change in Failure Stress on the Southern San Andreas Fault System Caused by the 1992 Magnitude = 7.4 Landers Earthquake*, Science *258*, 1328–1332.

TODA, S., STEIN, R.S., REASENBERG, P.A., and DIETERICH, J.H. (1998), *Stress Transferred by the* $M_w = 6.9$ *Kobe, Japan, Shock: Effect on Aftershocks and Future Earthquake Probabilities*, J. Geophys. Res. *103*, 24,543–24,565.

TRUESDELL, A.H. and LIPPMANN, M.J. (1990), *Interaction of Cold-water Aquifers with Exploited Reservoirs of the Cerro Prieto Geothermal System*, Geothermal Resources Council Trans. *14*, 735–741.

TRUESDELL, A.H., LIPPMANN, M.J., GUTIÉRREZ, P.H., and J. DE LEÓN, V. (1998), *The Importance of Natural Fluid Recharge to the Sustainability of the Cerro Prieto Resource*, Geothermal Resources Council Trans. *22*, 529–536.

WALSH, J.B. (2002), *Subsidence above a Planar Reservoir*, J. Geophys. Res. *107*, B9.

YANG, X. and DAVIS, P.M. (1986), *Deformation due to a Rectangular Tensional Crack in an Elastic Half-space*, Bull. Seismol. Soc. Am. *76*(3), 865–881.

(Received July 15, 2004; accepted November 20, 2004)
Published Online First: June 17, 2005

To access this journal online:
http://www.birkhauser.ch